Volume 3
Number 4
April 2025
Pages 1587–1984

RSC Sustainability

rsc.li/rscsus

ISSN 2753-8125

PAPER

Pratheep K. Annamalai, Ashok Kumar Nanjundan, Darren J. Martin *et al.*
Sustainable carbon for energy storage applications: investigation on chemical refinements of sorghum biomass for tuneability of carbon structures and supercapacitor performance

ROYAL SOCIETY OF CHEMISTRY

RSC Sustainability

ROYAL SOCIETY OF CHEMISTRY

PAPER

View Article Online
View Journal | View Issue

Cite this: *RSC Sustainability*, 2025, **3**, 1691

Sustainable carbon for energy storage applications: investigation on chemical refinements of sorghum biomass for tuneability of carbon structures and supercapacitor performance†

Rana Arslan Afzal,[a] Pratheep K. Annamalai, *[bc] Mike Tebyetekerwa,[a] Paulomi (Polly) Burey,[cd] John Bell,[f] Ashok Kumar Nanjundan *[ce] and Darren J. Martin *[a]

Biomass-derived carbon is a promising sustainable material for energy storage applications, but the correlation between biomass precursor characteristics and the resultant carbon's features and its electrochemical performance is not yet well defined. This study establishes a link between sorghum biomass characteristics such as lignocellulosic composition and morphology and derived carbon features, particularly its surface area, porosity, and specific capacitance. By systematically adjusting the biomass composition through chemical refinements, we demonstrate that cellulose-rich precursors lead to carbon structures with higher porosity and surface area, resulting in improved electrochemical performance. The carbon produced from water-washed sorghum biomass exhibited a specific capacitance of 54 F g^{-1}, on par with commercial activated carbon. A mild alkali treatment (2% w/v NaOH) of the biomass partially removed non-cellulosic components, enhancing the surface area and capacitance of the resultant hard carbon. Additional refinement through bleaching further removed hemicellulose and lignin, increasing the precursor's crystalline cellulose content. The carbonisation of this cellulosic precursor yielded carbon with higher porosity and surface area. These refinements yielded hard carbon with high specific capacitance values (98 F g^{-1} for a current density of 0.2 A g^{-1}). Activating the biomass-derived carbon further improved its specific capacitance by 70%, reaching 140 F g^{-1} at a current density of 0.2 A g^{-1} while maintaining 100% stability over 5000 cycles. Overall, this research establishes a favourable link between the electrochemical characteristics of biomass-derived hard carbons in supercapacitors and their cellulose content. In contrast, other non-lignocellulosic components, such as hemicellulose and lignin, adversely affect these characteristics. These findings provide groundwork for maximising the potential of carbon materials sourced from biomass by systematically fractionating primary biomass plant cell wall components.

Received 14th September 2024
Accepted 3rd December 2024

DOI: 10.1039/d4su00569d

rsc.li/rscsus

Sustainability spotlight

Sustainable carbon materials derived from renewable biomass sources offer an environmentally friendly alternative to non-renewable carbon materials. By demonstrating the use of agricultural biomass residues, such as sorghum stems, for carbon production, we show a pathway to reduce reliance on fossil fuels and decrease the environmental impact of carbon material synthesis. Moreover, the carbonisation of biomass involves lower energy consumption and minimises hazardous by-products compared to traditional methods. This research highlights how systematic chemical refinements of biomass components, such as cellulose, hemicellulose, and lignin, can optimise carbon properties for energy storage applications, providing a pathway to create high-performance, sustainable energy storage devices.

[a]*School of Chemical Engineering, The University of Queensland, St Lucia, Queensland 4072, Australia. E-mail: darren.martin@uq.edu.au*

[b]*School of Agriculture and Food Sustainability, The University of Queensland, St Lucia, Queensland 4072, Australia. E-mail: pratheep.annamalai@unisq.edu.au*

[c]*Centre for Future Materials, University of Southern Queensland, Toowoomba, Queensland 4350, Australia. E-mail: ashok.nanjundan@unisq.edu.au*

[d]*School of Agriculture and Environmental Sciences, University of Southern Queensland, Springfield, Queensland 4300, Australia*

[e]*School of Engineering, University of Southern Queensland, Springfield, Queensland 4300, Australia*

[f]*Deputy Vice-Chancellor's Office (Research & Innovation), University of Southern Queensland, Springfield, Queensland 4300, Australia*

† Electronic supplementary information (ESI) available. See DOI: https://doi.org/10.1039/d4su00569d

Introduction

Carbon is a crucial element in materials science and has been utilised as a raw material in many applications due to its adaptability and abundance. In particular, carbon materials structured at micro- and nanoscales exhibit electrochemical functionalities and are used in clean energy storage, carbon capture, water purification, and agriculture applications.[1] In recent decades, new sustainable and economical sources of carbon precursors have been explored to meet the increasing market demand for novel and advanced carbon-based materials.[2] Biomass-derived hard carbons have the potential for supercapacitor use, with plant-based biomasses being more practical due to their cost and abundance[3] compared to those produced from other sources.[4]

Contemporary research on utilising biomass carbon for energy storage applications focuses on transforming crops and fruit residues and pyrolysing the whole biomass under various carbonisation conditions and by activation strategies.[5–7] Particularly for supercapacitors, the wide pore size distribution has been shown to play a crucial role in enhancing the electrochemical performance of electric double-layer capacitor (EDLC) type supercapacitors. Other strategies to improve performance included incorporating pseudocapacitive materials to increase energy density and cycle stability.[7]

As a result, much prior research was carried out on turning plant-based biomasses into functional carbon materials by carbonisation.[3] This thermochemical process increases carbon content by eliminating other components. Yet, even within the classification of plant-based biomasses, the physicochemical and electrochemical characteristics of the produced carbon compounds vary significantly depending on the chemical composition of various biomass precursors, chemical and mechanical pre-treatment methodologies, and catalysts utilised. Prior research found that hard carbon compounds generated from plant-based biomass had varying specific capacities and cycling performances in supercapacitors.[3] It is commonly understood that the chemical composition of biomass is undoubtedly one of the determining factors for such a dramatic divergence.[8]

Generally, plant-based biomasses consist of lignocellulosic components, proteins, lipids, soluble extracts, and various inorganic minerals,[9] with lignocellulosic components (cellulose, hemicellulose, and lignin) comprising the bulk of the total weight.[9] Cellulose is a homopolysaccharide composed of anhydro-glucan units held together by β-(1,4)glycosidic linkages.[9] The molar mass of cellulose may vary depending on its biological origin and polymerisation level.[9] Hemicellulose and lignin are more complicated due to the heterogeneity of their component monomers. Hemicellulose has a complex structure composed of linear or branching polysaccharides generated from hexose (mannose, galactose, and glucose) and pentose (xylose and arabinose) monosaccharide units.[9] Similarly, the physicochemical characteristics of lignin are determined by the fraction ratios of three monomer units: *p*-hydroxyphenyl (H), guaiacyl (G), and syringyl (S).[9] Since these components exhibit different physicochemical properties and thermal decomposition behaviour,[9] their assembly in biomass with other non-lignocellulosic components and morphology significantly influence carbonisation behaviour.

Biomass features can be efficiently utilised by overcoming its inherent recalcitrant structure through chemical treatments commonly known as the pulping/delignification process, which uses various chemicals and mechanical treatments. For instance, an alkaline treatment enhances fibre swelling by disrupting the hydrogen bonds between hemicellulose and cellulose, breaking the xylan chain [9]. It also disturbs the connections between hemicellulose and lignin by cleaving the uronic and acetic esters and the ether and ester bonds.[9] Consequently, the hemicellulose component may be separated and dissolved. Additionally, bleaching treatment is performed to remove lignin from the lignocellulosic biomass. Due to several chemical components in the cell wall, the bleaching process may be complicated. However, it often involves oxidation and/or chlorination reactions. In short, sodium chlorite decomposes to chlorine dioxide under aqueous acidic conditions, which bleaches through the radical process.[9] The influence of these chemical treatments has been investigated in the context of cellulose nanofibre (CNF) research.[9] However, it has yet to be expanded and explored to assess the full implications of carbonised material properties.

During carbonisation, cellulose, hemicellulose, and lignin are degraded at various temperatures *via* their specific routes, kinetics and complicated interactions with other components (*e.g.*, minerals) to create char structures.[10] Each lignocellulosic component undergoes a unique degradation route to achieve its chemical destination, influenced by thermochemical treatment variables such as holding temperature and heating rate.[11] Hemicellulose and cellulose respond differently when subjected to a thermochemical treatment because their breakdown temperatures and routes vary.[12] Hemicellulose tends to depolymerise and break down at a lower temperature (300 °C), while cellulose needs a higher temperature (400 °C) owing to its more crystalline structure.[13] Conversely, lignin has an entirely amorphous structure with strongly crosslinked polymeric monomer units of aromatic rings, resulting in a broad range of thermal breakdown temperatures and sluggish reaction kinetics.[13]

Consequently, altering the proportions of these three lignocellulosic components would significantly modify the reaction intermediates and kinetics, synthesising carbon compounds with very diverse characteristics. This provides an opportunity to design the carbon structure by tuning the lignocellulosic composition of plant biomasses. At the same time, some pioneering research has sought to determine the compositional impacts of biomasses on the energy storage capability of biomass-derived hard carbons by comparing various entire biomass precursors.[14] Nevertheless, it is still unclear how each specific component, particularly the primary components of biomass, *i.e.* cellulose, hemicellulose, and lignin, affects the resultant carbon characteristics and the electrochemical performance of the supercapacitor. To this end, as an example, we investigated agricultural residues of sorghum biomass as a nonwood lignocellulosic source[15,16] for producing advanced

carbon materials. This biomass offers numerous benefits, including its renewability, cost-effectiveness, and harvestability in semi-arid or arable lands, with the biomass yield ranging from ~10 to 48 Mg ha^{-1}.[17] It also offers versatile lignocellulosic composition and morphology[15,16] that can be engineered to produce diverse carbon materials. Its utilisation in advanced materials applications is advocated for increasing regional bioeconomy by increasing economic value, creating jobs, and promoting self-sufficiency.[18–20]

Our previous work demonstrated how lignocellulosic composition and morphology variations within different plant parts (leaf, sheath and stem) of sorghum biomass affect the carbon structure and properties, resulting in improved electrochemical performance.[15] Herein, we present for the first time a chemical refinement method to change the main composition of biomass to elucidate the roles of specific biomass components in defining the structural and electrochemical characteristics of hard carbons. For this, the stem part of the sorghum biomass was chosen and three different chemical (mild and harsh alkaline delignification and bleaching) refinements were performed to vary its lignocellulosic composition and morphology. These treatments were explored as mild chemical pretreatments for nanocellulose production at low energy consumption.[9,21] The influence of these treatments on the features (such as surface area, graphitisation, porosity, particle size and yield) of derived carbon is correlated with the performance of supercapacitors prepared with these carbon materials. The newly acquired information will aid in the sensible selection and fractionation of plentiful and sustainable biomass for energy storage applications.

Results and discussion

Lignocellulosic composition

Chemical refinements of sorghum biomass were conducted to modify the lignocellulose content and remove extractives. Water-washed (WW), 2% w/v NaOH treated (2DL), 10% w/v NaOH treated (10DL), and 2% w/v NaOH treated and bleached (2DL + BL) samples were prepared. Fig. 1(a) exhibits the chemical composition analysis of the cellulose, hemicellulose, lignin, ash, and extractives. The lignocellulose content of sorghum biomass was evaluated after the chemical refinements. The current approach simplifies the estimation by accounting for cellulose as the glucan, hemicellulose as the total of the remaining glycans, and lignin as Klason and acid-soluble lignin. This is a popular method of reporting chemical composition data in the scientific literature.[9] Table 1 provides detailed information on lignocellulosic composition (glucan, xylan, arabinan, mannan, Klason lignin- and acid-soluble lignin, ash, and extractives). The lignocellulosic composition of the water-washed sorghum was cellulose (24 ± 2%), hemicellulose (9 ± 1.5%), lignin (14 ± 1.8%), extractives (37 ± 1.4%), and ash (5 ± 1.4%). The details of this water-washed sample of the upper stem of the sorghum plant are presented in our previous work.[15] Additionally, these results are supported by J. Pennells *et al.* previous work.[16]

After water washing, the first refinement of sorghum biomass powder was accomplished by treating it with a 2% w/v NaOH solution at 80 °C for 2 hours and labelled as 2DL. Based on prior studies involving non-wood biomass such as arid spinifex grasses, this procedure is an adequate baseline

Table 1 Details of lignocellulosic composition of water-washed and chemically refined sorghum samples

	WW		2DL		2DL + BL		10DL	
	Pre.	SD	Pre.	SD	Pre.	SD	Pre.	SD
Total sugars	38.7	2.4	82.1	2.5	81.7	2.4	83.3	2.7
Glucan	24.1	2	55.5	2.1	63.9	1.7	76.8	2
Xylan	13.1	0.8	22.8	0.5	16.4	0.6	4.5	0.7
Mannan	0.01	0.2	0.4	0.2	0.2	0.2	0.08	0.1
Arabinan	1.3	0.3	2	0.3	1.4	0.3	0.6	0.3
Galactan	0.5	0.2	0.5	0.1	0.2	0.1	0.2	0.1
Rhamnan	—	—	0.1	0.08	—	—	—	—
Klason lignin	11.5	1.5	11	1.4	10.7	1.4	12.4	1.6
Acid soluble lignin	1.6	0.3	1.34	0.2	1.66	0.2	1.05	0.3
Ethanol extractives	37	1.4	0.5	0.8	0.4	1	2.1	1.1
Ash	3.1	1.4	1.1	1	0.2	0.7	1	1.1
Acid insoluble ash	1.1	1	0.3	1	0.1	0.7	0.5	1
Acid insoluble residue	12.6	2	11.5	2	9.8	2.1	13.1	2.1

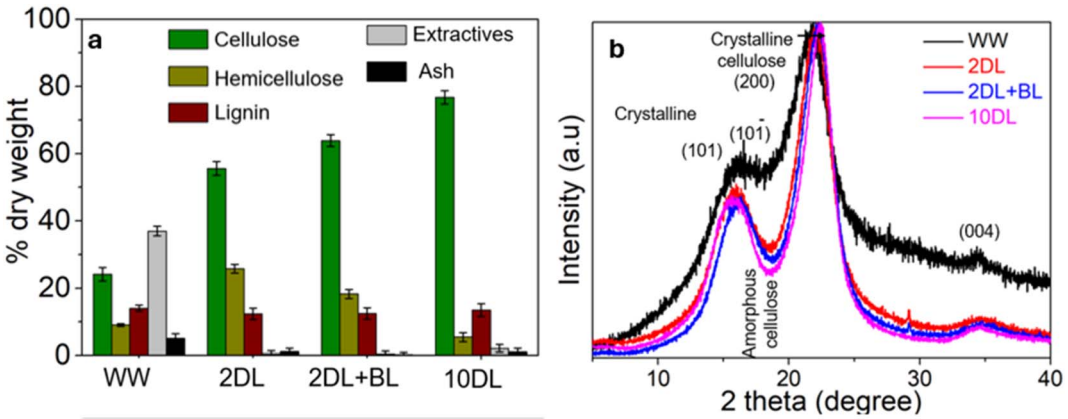

Fig. 1 (a) Lignocellulosic composition, and (b) XRD of WW and chemically refined sorghum and derived carbon samples.

approach for removing extractives and waxy components without affecting other components and maintaining a high yield.[22] Usually, the mild alkali treatment led to partial fibrillation and the opening or loosening of the fibre bundle's structure, resulting in the dissolving of soluble lignin and the breakdown of the link between hemicellulose and lignin. Consequently, it dramatically decreased the quantity of extractives, including sugars, compared to only water washing. As expected after the elimination of extractives, the relative amounts of cellulose, hemicellulose, and lignin in the delignified sample increased.[9] 2DL treatment eliminated most of the extractives with only a $0.5 \pm 0.8\%$ amount detected in the pulp.

Additionally, a significant amount of ash was removed after 2DL refinement, where only $1.09 \pm 1\%$ of ash was measured. This treatment also reduced the lignin content. This happens *via* cleavage processes in which hydroxide anions (OH) break α-aryl ether and β-aryl ether bonds, separating lignin macromolecules into fragments that may be readily dissolved in aqueous alkali environments.[21] In the scientific literature, alkaline solutions at high temperatures often remove lignin from biomass.[21] Since non-wood biomass sources have less lignin and "softer" lignin in their cell walls than wood, it is generally possible to perform pulping under much milder conditions.[9] Lignin and resin are highly hydrophobic components of sorghum, which may prevent cellulose from swelling and obstruct subsequent structural component removal and nanofibre isolation procedures. Therefore, their removal and the associated loosening of the plant's fibrous structure by alkali treatment are required before further chemical and mechanical refinements. According to Fig. 1(a), pulping with 2DL increased the cellulose from 24% to 55% and hemicellulose from 15% to 25%. This is due to the extensive removal of extractives from 37% to 0.5% and the slight removal of lignin, raising the relative quantity of cellulose and hemicellulose in the delignified or pulped sample.

The mild delignified sample (2DL) was treated further through sodium chlorite bleaching treatment, and the resulting sample was denoted as 2DL + BL. During this bleaching process, which was performed twice, extractives and ash were further removed from the 2DL sample. Additionally, the hemicellulose content decreased to 18% due to the susceptibility of xylan to chemical degradation during chlorine oxidation. As a result of the reduction in extractives and hemicellulose, the cellulose content increased to 64%. Notably, the lignin content remained essentially unchanged following bleaching. A similar behaviour was observed by B. Sharma *et al.* in their work on bamboo bleaching.[23] This phenomenon could be attributed to lignin condensation, or the lignin in the 2DL pulp remains particularly recalcitrant (resistant) to mild bleaching reactions using 1% w/v $NaClO_2$. Although the bleaching process may cause cell wall breakage and partial oxidation of lignin (as indicated by the visible colour change in chromophoric groups), the lignin polymers are not entirely solubilised or eliminated; instead, they undergo condensation and remain detectable.[23] Lignin condensation has long been a persistent concern in traditional and modern manufacturing industries, prompting numerous efforts across various fields to address this issue.[24]

The '10DL' treatment of sorghum involved using a 10% w/v NaOH solution to remove hemicellulose from the biomass. This approach was chosen based on previous studies that efficiently extracted hemicellulose from various biomasses, including wood and non-wood.[9] As the concentration of NaOH increased from 2DL (25.8% hemicellulose) to 10 DL (5.4% hemicellulose), the amount of hemicellulose decreased. Hemicellulose components were hydrolysed and washed away[9] during this process, increasing cellulosic content. The α-cellulose content increased from 55% to 76% following treatment with 10% w/v NaOH (Fig. 1(a)). This increase is attributed to removing hemicellulose surrounding other plant components, raising the relative quantity of cellulose in the pulped or delignified sample. These findings suggest that some more easily accessible hemicelluloses are degraded and/or dissolved in the alkaline media. It is known that the alkaline treatment at higher temperatures (over 100 °C) may promote scission of the reducing end group of hemicellulose. However, earlier research has also demonstrated that even modest NaOH treatment (0.5–2%, 30–60 °C) of other species results in a drop in hemicellulose content, similarly ascribed to its breakdown.[9] This finding demonstrated that sorghum biomass can be processed to obtain a comparably cellulose-rich pulp through alkali treatment under harsh conditions. An alkaline treatment of sorghum with 10% NaOH slightly increased the lignin concentration, possibly due to the condensation of residual lignin or the creation of lignin carbohydrate complexes on the fibre's surface.[21] This phenomenon of lignin condensation was also observed by A. Hosseinmardi *et al.* during the alkaline delignification of spinifex grass biomass at higher NaOH concentrations,[21] attributing to the re-polymerisation of lignin.[24] These findings have demonstrated that a series of systematic chemical refinements of a single sorghum biomass can be performed in a controlled manner that alters the lignocellulose composition. As postulated earlier, the variations in the lignocellulosic composition will significantly influence the derived carbon features, and the carbonisation behaviour was further evaluated.

X-ray diffraction (XRD) analysis

Fig. 1(b) displays the X-ray diffractograms of sorghum WW and chemically refined samples. The well-defined peaks can be detected at 2θ values of 15.2°, 16.2°, 22.3°, and 34.5°, which correspond to the (101), (101), (200), and (004) planes of crystalline cellulose I, respectively.[21,25,26] The intensity of the 101 planes in the XRD patterns of chemically treated samples was similar to the signatures in the water-washed sample, indicating that the cellulose I crystal structure and crystalline order were largely unaffected by the chemical treatments. In contrast, the amorphous phase (disordered region), primarily observed at $2\theta = 18.5°$, showed a noticeable decrease in peak intensity with increasing chemical refinement. This is attributed to the removal of amorphous hemicellulose and lignin, as shown in Fig. 1(a).[21]

The degree of crystallinity (CrI) for each sample was determined using the method proposed by Segal *et al.*[27] The water-

washed (WW) sample exhibited the lowest crystallinity, with a CrI of 41 ± 1.9%, likely due to the significant presence of amorphous hemicellulose and lignin. Following 2DL treatment, the CrI value increased to 66.5 ± 0.5% and further increased to 71.2 ± 0.8% after bleaching. The 10DL sample exhibited a CrI value of around 76.5 ± 1.7%, the highest measured value among samples. This increase in crystallinity after chemical refinements is associated with the removal of amorphous plant cell wall components, particularly hemicellulose and lignin, while preserving the crystalline cellulose I phase in the biomass. Therefore, these chemical refinements eliminated substantial quantities of amorphous material without affecting the crystalline phase of cellulose I.

Fig. S1(a)† presents the XRD patterns of carbonised sorghum samples. Upon carbonisation at 1000 °C, the diffraction peaks at 15.2°, 16.2°, and 22.3° disappear, while two peaks emerge at 21° and 43.8°, corresponding to the (002) and (101) reflections of typical turbostratic carbon structures. This reveals that sorghum samples are carbonised well and hard carbon is developed. Notably, the peak at 21° of the carbon samples from 2DL treatment is broader than that of the water-washed (WW) sample, indicating a lower degree of graphitisation. This is probably due to the removal of heteroatoms by 2DL treatment, which potentially function as nucleation sites for graphene domain creation.[28]

Additionally, a small hump near 28°, which corresponds to a graphitic plane, emerged in the 2DL + BL sample, becoming pronounced in the 10DL sample.[29] The development of this peak suggests that carbon is becoming increasingly graphitic,[30] a well-known characteristic enhancing in-plane conductivity necessary for electrochemical applications.[31] A similar peak was reported by M. Sivachidambaram *et al.*,[32] which gradually increased with the increase in carbonisation temperature. However, in the current study, temperature is kept constant, suggesting that this peak is likely associated with removing hemicellulose. This hypothesis is further corroborated by Raman spectroscopic analysis.

Raman spectroscopy

As shown in Fig. S1(b),† two separate carbon bands are examined at 1340 cm^{-1} and 1585 cm^{-1}, corresponding to the D band (disordered sp^3 carbon) and the G band (ordered sp^2 carbon). The I_D/I_G values for WW, 2DL, 10DL and 2DL + BL samples are 0.92 ± 0.01, 0.96 ± 0.01, 0.89 ± 0.007 and 0.93 ± 0.001, respectively. The WW sample showed a relatively low I_D/I_G value, while the 2DL (after eliminating extractives, resin, and minerals) resulted in an increased I_D/I_G value. This rise may be due to alterations in the native crystalline structure of cellulose fibrils compared to chemically untreated WW-C samples. In contrast, the 10DL sample showed a significant decrease of I_D/I_G for 10DL, possibly due to the elimination of hemicellulose. Hemicellulose is a polymer composed of heterogeneous monosaccharide units (arabinoxylans, arabinogalactans, β-glucans, *etc.*).[33] Its thermal depolymerisation leads to degradation and ring rearrangement of these monosaccharides. Previous studies using TGA[34] have shown that hemicellulose degrades over a wide temperature range, reflecting the varying thermal stability of its monosaccharide units. This broad degradation range may hinder carbon rearrangement, resulting in a low proportion of sp^2 carbon structures.

In contrast, cellulose, consisting solely of β-glucose monomers, degrades within a narrower temperature range of 310–400 °C.[15] Upon carbonisation, this relatively homogeneous makeup could recombine carbon rings into carbon sheets with sp^2 configurations. Furthermore, with its extensive crosslinked structure, lignin is a relatively more thermally resistant component. It degrades at higher temperatures, from 200 °C to 900 °C.[35] Due to the slower kinetics of its thermal degradation, lignin may significantly inhibit the formation of sp^2 carbon structures.

Field-emission scanning electron microscopy (FESEM)

The influence of chemical refinements on the precursor's morphological features was examined using field-emission scanning electron microscopy (FESEM), and the results are presented in Fig. 2. The FESEM images reveal that after water treatment (WW), the microfibre bundles of sorghum biomass largely remain intact. In contrast, after chemical refinements, samples (2DL, 10DL and 2DL + BL) show ruptured and porous morphologies of biomass, indicating breakage of chemical connections between the lignocellulosic components in the sorghum cell wall. Also, these samples exhibit reduced fibre/particle size, indicating physical rupture and partial fibrillation.

First, the delignification by alkali treatment (2DL) effectively eliminated non-fibrous components (extractives, mineral ash, and any resin) from the surface and partially from the bulk of the fibre bundles. Under this mild alkali condition, the microfibres lose the thick fibre morphology and become smaller. The 10DL refinement more intensively removes the hemicellulose and lignin at a higher alkali concentration, disrupting the bundle morphology and facilitating fibrillation and porous structure (vascular morphology). Subsequent bleaching treatment on the 2DL pulp further enhances defibrillation, resulting in a more significant number of microfibres for the 2DL + BL sample.[36] Moreover, the microscopic images of these chemically refined samples also show that the elimination of extractives becomes increasingly apparent when sorghum samples are chemically refined (2DL < 2DL + BL < 10DL), and this elimination of extractives leaves pores. Such porous morphology was not observed in the WW sample.

These four types of sorghum samples were then subjected to carbonisation at 1000 °C under a nitrogen atmosphere, and the FESEM images of the resulting carbon samples are shown in Fig. 2. The FESEM images reveal substantial morphological variations, notably in the size of individual particles. Water-washed, delignified, and bleached sorghum-derived carbons have shown a tendency to decrease the size of individual carbon particulates significantly. This indicates that the different extents of morphological disruption and defibrillation of samples upon chemical refinement are significant factors in determining the size and shape of the resulting carbon

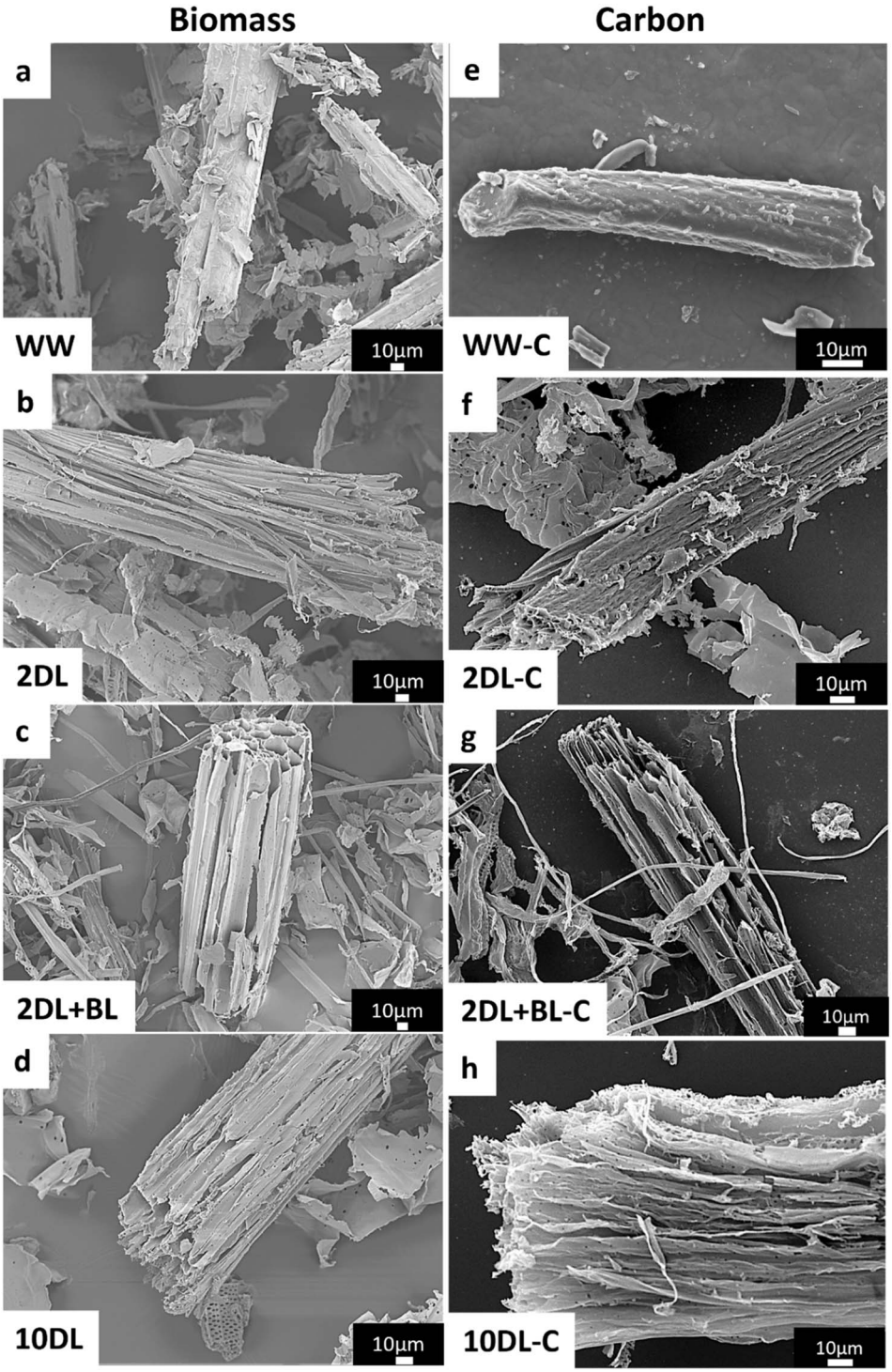

Fig. 2 FESEM images of (a) water-washed and (b–d) chemically refined sorghum biomass and (e–h) carbonised samples.

materials.[36] Hence, chemical refinements of biomass offer potential control over the morphology and porosity of derived carbon.

Carbonisation behaviour

Fig. 3(a) depicts the TGA% mass loss graphs from 40 to 500 °C and Fig. 3(b) shows their related first derivative of the mass change (DTG) curves. The TGA curves exhibit three distinct stages. In the first stage, occurring between 40 °C and 150 °C, the weight loss is ascribed to the rupture of water-lignocellulosic linkages or removal of molecular water from cellulosic components.[15] Following dehydration, the biomass undergoes complicated processes, including the degradation of carbohydrates and lignin. Amorphous materials such as

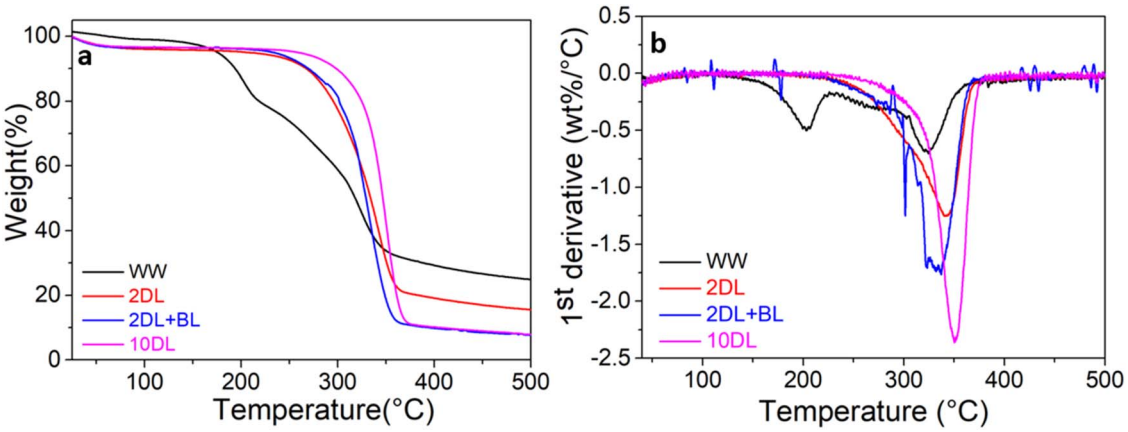

Fig. 3 (a) TGA and (b) DTG thermograms for water-washed and chemically treated sorghum samples in a nitrogen environment.

hemicellulose (*i.e.*, xylose, mannose, galactose, and glucose) depolymerise in the second stage, which occurs between 150 °C and 315 °C.[15] Additionally, lignin decomposition starts in this range but continues over a very broad temperature range and at a very modest mass loss rate.[15]

The TGA and DTG curves in this temperature regime revealed that the water-washed sample experiences the most significant mass loss among all the samples, with decomposition beginning around 150 °C and reaching a peak at 204 °C as displayed in DTG. The presence of a high amount of extractives (Fig. 1(a)), which are low in molecular weight and highly volatile, is one of the reasons for the poor thermal stability of the water-washed sample.[15] The chemically refined samples exhibit enhanced thermal stability associated with removing extractives and hemicellulose. This phenomenon is particularly evident in the 10DL sample. An improvement in thermal stability of the 10DL sample has been distinctly higher than that of the other samples, which can be attributed to the removal of hemicellulose and extractives. This sample has also exhibited relatively higher lignin content.

The final stage of thermal decomposition occurs above 315 °C, where most decomposition corresponds to cellulose breakdown. The TGA curves reveal higher onset degradation temperature for all chemically refined samples. Additionally, the DTG curves show the temperature of maximum weight loss (T_{max}) for each sample within the same range, between 326 and 354 °C. This indicates that the cellulose degradation rate is consistent with the chemical treatment concentration and cellulose content. The first derivative of weight loss (dTGA/dT) for the water-washed sample occurred at −0.67 wt%/°C, and it increased to −2.3 wt%/°C for the sample treated with 10% w/v NaOH.

Several studies have shown that lignin decomposition occurs over a range of temperatures from around 200 °C to as high as 700 °C.[21] Lignin is typically associated with high thermal stability due to its thermally stable aromatic structures. Beyond 375 °C, the TGA curve transitions from a sharp decrease to a more gradual slope, indicating slower mass loss up to 500 °C. The final mass loss, occurring above 375 °C, is ascribed to the breakdown of remaining lignin. The residual mass at 500 °C for WW is 24.6 wt%, which decreases to 15.6 wt% for 2DL and reduces further to 7.6 and 8 wt% on 2DL + BL and 10DL, respectively.

These findings suggest that chemical refinements have modified biomass precursors' lignocellulosic composition and fibre morphology, leading to distinct thermal behaviours. Three primary factors contribute to this phenomenon. First, chemical refinements facilitate the removal of more amorphous structures (*e.g.*, extractives and hemicellulose) during alkaline treatment. Second, XRD analysis indicates that chemically refined samples exhibit more ordered crystalline areas with less polymeric disorder or amorphous structure. This increased degree of crystallinity (Crl) predictably enhances the material's thermal stability, requiring higher temperatures for degradation.[21] Third, the loss in thermal stability was also attributable to a reduction in particle size and, thus, an increase in surface area, which permits more rapid thermal disintegration.[37]

The influence of the particle size and surface area on the thermal stability of chemically treated fibres is also correlatable. The 2DL + BL sample, with its smaller particle size and highest surface area, exhibits lower thermal stability and faster degradation (lower T_o and T_{peak}) than other chemically treated samples. In contrast, the 10DL sample has a larger partial size and a lower surface area than the 2DL sample, so it has higher thermal stability. Overall, these chemical refinements of biomass precursors significantly influence their carbonisation behaviour or offer the potential to modify the carbon structures. Also, the water-washed sample was excluded from further electrochemical studies due to its potential to contain significant contaminants (during growth and harvest).

Surface chemistry (X-ray photoelectron spectroscopy)

Table 2 presents the relative mean of elemental atomic percentages on the surfaces of the samples, and Fig. S2 and S3† show the deconvolution using X-ray photoelectron spectroscopy (XPS). The XPS analysis reveals that carbon and oxygen are the predominant surface elements, with trace amounts of nitrogen and silicon. Silicon presence occurs naturally in crops since it is

Table 2 X-ray photoelectron spectroscopy (XPS) survey scan and high-resolution carbon X-ray photoelectron spectroscopy (HR XPS) spectra details for water-washed and chemically refined sorghum and associated derived carbon samples

Sample	Elemental and bonding characteristics	WW		2DL		2DL + BL		10DL	
		at%	SD	at%	SD	at%	SD	at%	SD
Biomass samples after chemical refinement	O	29	0.5	34	0.1	37	0.3	36	0.3
	C	69	0.6	65	0.4	63	0.5	64	0.3
	N	1.6	0.2	0.4	0.1	—	—	—	—
	Si	0.5	0	—	—	—	—	—	—
	C1 (C–C, C–H)	50	0.3	26	0.9	18	1	14	0.2
	C2 (C–O–C, C–O)	39	0.8	58	0.8	62	0.3	54	1
	C3 (C═O)	9.3	0.8	14	1.2	20	0.7	31	0.8
	C4 (COOH)	2.3	0.1	2	1	—	—	—	—
Carbonised samples	O	7.7	0.3	8	2	3	0.1	4	0.4
	C	91	0.5	92	3	97	0.3	96	0.2
	Si	0.8	0.2	—	—	—	—	—	—
	C–C	49	0.1	23	0.06	49	0.1	54	0.2
	C–O–C	24	0.01	28	1.5	5	0.2	4	0.1
	C–O	39	1.6	37	0.2	27	0.1	23	0.04
	π–π	4	0.01	13	0.1	19	0.2	19	0.1

taken up by plant roots in the form of silicic acid and subsequently deposited in cell wall structures such as amorphous silica, hydrated silica, and silicate. In the WW sample, the atomic percentage of silicon is 0.5%, and that of nitrogen is 1.6%. Following mild chemical refinements, silicon is removed, and the amount of nitrogen is decreased, with both elements disappearing entirely after more intensive chemical treatments.

Table 2 presents the high-resolution C 1s spectra for WW and chemical refinements of sorghum biomass samples. The C 1s spectra can often be described in four principal peaks classified into C1, C2, C3 and C4. The C1 peak is allocated to the C–C and C–H groups, C2 is linked to C–O groups, C3 is associated with O–C–O and/or C═O groups, and C4 corresponds to the COOH group (carboxylic acid or ester).[3] The C1 peak, at around 285 eV binding energy, correlates to aromatic and aliphatic carbon backbones, representing non-cellulosic components identified as adventitious carbon, lignin, and extractives.[21] The intensity of this peak for the WW sorghum is 49 ± 0.3%, which decreased upon chemical refinements to 26 ± 0.9, 18 ± 1, and 14.5 ± 0.2% for 2DL, 2DL + BL and 10DL treatments, respectively. This suggests the removal of adventitious carbon and extractives (such as resins and fatty acids).

The C2 peak, near 286 eV binding energy, is associated with cellulose and hemicellulose.[21] The intensity of this peak increases after chemical refinements. The C3 peak, near 288 eV binding energy, corresponds to C═O and O–C–O functional groups, which may be associated with the carbonyl groups of lignin or extractives.[21] The fourth peak (C4) near 298 eV binding energy might originate from ester linkages in lignin and carboxylic acid groups of uronic acids in hemicellulose. As the chemical refinements gradually remove lignin and hemicellulose, the C4 components are eliminated by intensive chemical refinements.

XPS analysis was further used to examine the surface chemistry of the biomass-derived carbon samples. As noted in Table 2, carbonisation significantly increased the carbon content while markedly reducing oxygen content in carbonised samples. This change is attributed to the carbonisation process, which removes oxygen and other volatile components, as explained in the TGA section. The WW-C shows 91 ± 0.5 of carbon and 7.7 ± 0.3 at% of oxygen. As the level of chemical refinement increases such as 2DL, 2DL + BL, and 10DL, the atomic percentage of carbon increases to 92 ± 3, 97 ± 0.3, and 96 ± 0.2 at%, respectively, while the oxygen content decreases to 8 ± 2, 3 ± 0.1, and 4 ± 0.15 at%, respectively.

The high-resolution XPS spectra of carbon samples for C 1s (Table 2) were also deconvoluted into four peaks at 284, 286, 287, and 290 eV, which can be attributed to C–C, C–O–C, C═O, and π–π (satellite of sp^2 carbon) respectively.[36,38] According to the data in Table 2, the 10DL sample exhibited the highest concentration of C–C sp^2 bonds (54%), corresponding to its lowest I_D/I_G peak ratio in the Raman spectra. All carbon samples contained a certain proportion of oxygen-bonded carbon groups, including C–O and C═O groups, which are potentially redox-active and contribute to significantly improved wettability. These increased the number of chemically reactive sites and enhanced overall specific capacitance.[39] These changes were earlier demonstrated by varying carbonisation temperatures.[3] However, this study indicates that systematic chemical refinement can achieve similar results while maintaining constant carbonisation conditions.

Nitrogen adsorption–desorption isotherms

The samples were evaluated using the N_2 adsorption–desorption method to examine the porosity development resulting from chemical refinements. As shown in Fig. S4(a),† the analysis reveals the presence of micropores and mesopores of varying sizes. The increasing adsorption volume at low relative pressure (0–0.2) indicates the existence of micropores, while the desorption hysteresis at medium relative pressures (0.2–0.9)

Table 3 BET-specific surface area and pore diameter of water-washed and chemically refined sorghum-derived carbon samples

	BET-specific surface area ($cm^2\ g^{-1}$)	Pore diameter ($cm^3\ g^{-1}$)
WW-C	0.5	0.001
2DL-C	19	0.01
10DL-C	78	0.02
2DL + BL-C	88	0.05

indicates the presence of mesopores. The short tails at a relative pressure close to 1.0 (>0.9) indicate the presence of macropores.[39] The magnitude of hysteresis grows proportionally with more intensive chemical refinements. The carbon samples under relative pressures ranging from 0 to 0.9 exhibit Type I/IV mixed isotherms that show the hierarchical distribution of micropores and mesopores.

The specific surface area and pore volume of WW (0.5 $cm^2\ g^{-1}$ and 0.001 $cm^3\ g^{-1}$) increased significantly following chemical refinement, with values of 19 $cm^2\ g^{-1}$ and 0.01 $cm^3\ g^{-1}$ for the 2DL sample, 78 $cm^2\ g^{-1}$ and 0.02 $cm^3\ g^{-1}$ for the 2DL + BL sample and 88 $cm^2\ g^{-1}$ and 0.05 $cm^3\ g^{-1}$ for the 10DL sample (Table 3). This increase shows the potential for controlling carbon's surface area and pore volume. Such an increase was previously reported by modulating the carbonisation temperature.[3] However, this study demonstrates that it can also be accomplished while maintaining a constant carbonisation temperature.

The pore structure of carbon samples is further supported by the pore size distribution plots (Fig. S4(b)†), which were estimated using the Barrett–Joyner–Halenda (BJH) model. The chemical refinements of sorghum biomass generate more microporous structures in the carbon samples. The observed correlation between surface area and microporosity is directly linked with the cellulose content in the precursor. This is potentially associated with the changes in the internal structure of cellulose fibrils that occurred during chemical refinements and carbonisation. J. Deng *et al.*[11] reported that during carbonisation, large amounts of oxygen-containing functional groups in cellulose and hemicellulose are eliminated as H_2O, CO_2, and CO, resulting in micropores.

In contrast, rich in chemically inert aromatic units, lignin tends to form nonporous carbon materials.[40] The chemically refined precursors yield porous carbon structures with a higher surface area than the WW sample. Hence, it is plausible to deduce that the prudent selection of chemical refinements of any biomass precursor can systematically control the specific surface area and pore volume. It has been reported that the pore volume and specific surface area are directly associated with activation temperatures.[3] In this study, a direct correlation with the intensity of chemical refinement can also be seen.

Yield of chemically refined pulp and its carbon

In the context of pulping, the yield is a percentage of the dry-weight material left after each chemical treatment. While these values are reported as averages from multiple treatments, they should be interpreted as approximations rather than absolute values. The primary treatment of pulping sorghum biomass with 2DL at 80 °C for 2 hours eliminated over 45% of the raw feedstock material (by weight). However, more intensive treatment with 10DL under the same reactions recovered approximately 35% of the original feedstock material's weight. The yield of bleached pulp obtained from 2DL pulp was around 90%.

Following carbonisation at 1000 °C, the carbon yields were 25.6 ± 0.7%, 16.6 ± 1.5%, 11 ± 1.8%, and 12 ± 0.7% by weight for WW-C, 2DL-C, 10DL-C and 2DL + BL-C, respectively. These carbon yield values correlate with the cellulosic polymer content in the biomass precursors (Fig. 1). Higher cellulose content in biomass typically produces a lower carbon yield; this might be associated with the higher number of volatile components in cellulose. Notably, the 10DL and 2DL + BL treatments resulted in comparable yields of carbon, albeit with different carbon structures and porosities.

Electrochemical performance of carbon samples

To understand the influence of chemical refinements on the electrochemical properties, the supercapacitor performance of the carbon samples (WW-C, 2DL-C, 2DL + BL-C, and 10DL-C) derived from sorghum biomass after chemical refinements was evaluated by cyclic voltammetry (CV) and galvanostatic charge–discharge (GCD) measurements. A commercial sample of activated carbon (CAC) was evaluated under the same conditions as those of the control. To demonstrate the impact of the activation of biomass carbon, 10DL-C was further activated with KOH treatment, and the resultant sample (10DL-AC) was also tested for electrochemical performance. Fig. 4 and 5 present the CV and GCD curves for all the tested carbon samples, respectively, while Fig. 6 highlights the comparative performance of all samples at a specific scan rate and current density.

The CV curves (Fig. 4) measured using a three-electrode setup at varying scan rates (of 5, 10, 20, 50, and 100 mV s^{-1}) in a potential range of −1 to 0 V show distinct rectangular shapes for all samples, indicating good capacitive behaviour with low resistance. The baseline sorghum-derived carbon 'WW-C' and the control sample 'CAC' exhibit comparable performance, suggesting that minimal chemical treatment (water washing) yields carbons with similar electrochemical properties to industrial-grade activated carbon. Then, the CV curves become progressively quasi-rectangular upon chemical refinements of biomass precursors. As compared in Fig. 6(a) at a specific scan rate (5 mV s^{-1}), the 10DL-C sample, derived from sorghum biomass treated with 10% NaOH delignification, showed enhanced electrochemical behaviour compared to its lower alkali-treated or bleached counterparts (2DL-C and 2DL + BL-C). This increased capacitance may result from the enhanced diffusion of electrolyte ions *via* densely interconnected hierarchical nanopores, reflecting increased surface area and pore volume of resulting carbons derived through chemical refinements and carbonisation.[3]

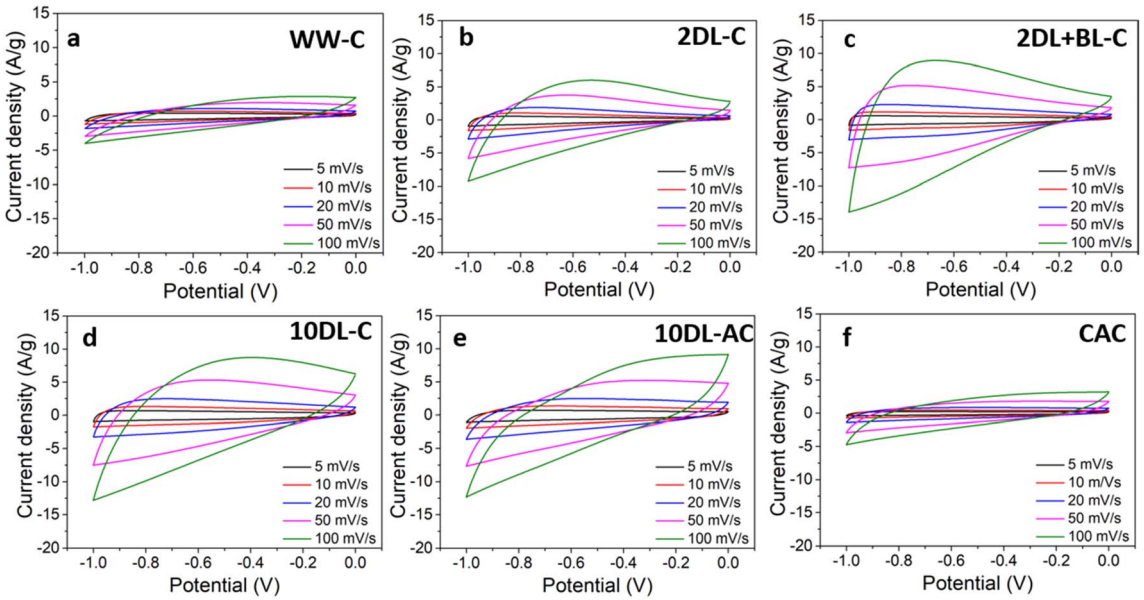

Fig. 4 Cyclic voltammetry analysis curves with electrodes prepared with carbon samples obtained from (a) water-washed and (b–d) chemically refined (e) KOH activated and (f) commercial activated carbon sample, at different scan rates.

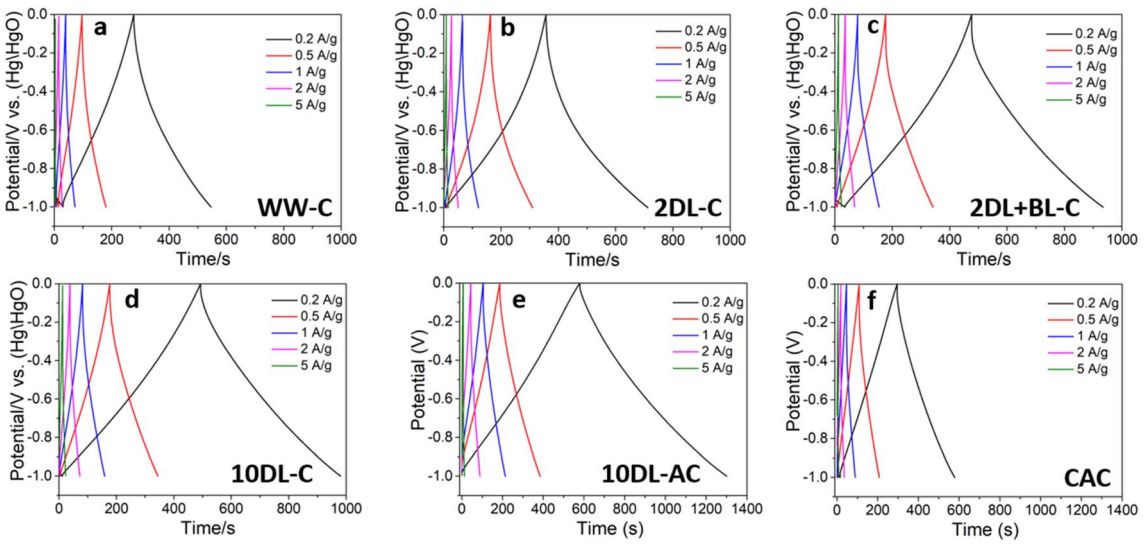

Fig. 5 Galvanostatic charge/discharge curves of the carbon samples obtained from (a) water-washed and (b–d) chemically refined (e) KOH activated and (f) commercial activated carbon sample, at current densities of 0.2, 0.5, 1, 2, and 5 A g^{-1}.

A similar trend can be observed in Fig. 5, which depicts the galvanostatic charge/discharge (GCD) curves of the samples at current densities of 0.2, 0.5, 1, 2 and 5 A g^{-1}. All the samples showed longer charge/discharge times at a low current density, indicating that the electrolyte ions have considerable time to enter and diffuse through carbon. The WW-C and CAC samples showed shorter and comparable charge/discharge times (Fig. 5). Among the carbon samples derived after chemical refinements, the 10DL-C sample exhibits the longest charge/discharge time demonstrating superior specific capacitance and lower internal resistance at various current densities. As compared in Fig. 6(b), 10DL-C exhibited a nearly triangular GCD curve with minimal IR drop, indicative of efficient charge–discharge behaviour.

The specific capacitance of electrodes at different current densities was also estimated from GCD measurements and is presented in Fig. 6(c). The specific capacitance of WW at 0.2 A g^{-1} is 54 F g^{-1}, which is slightly lower than that of CAC (57 F g^{-1}). The relatively lower capacitance of the CAC sample can be attributed to two key limitations: (i) its abundant micropores that impede the electrolyte ions' access at high current densities and (ii) an intense amorphous carbon framework that lowers the electron conductivity and electrolyte stability, resulting in poor rate performances.[41] After mild

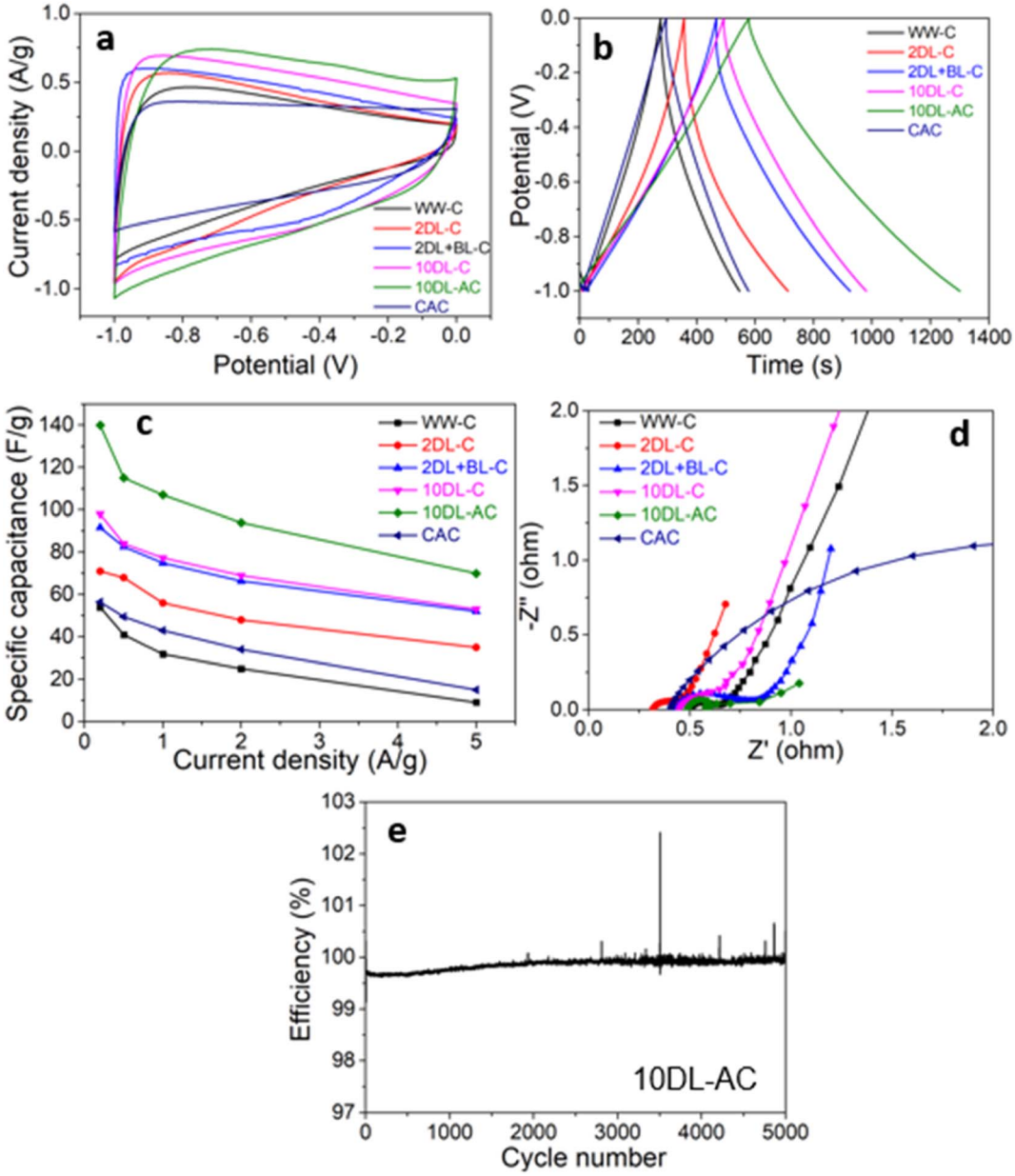

Fig. 6 (a) CV curves at a scan rate of 5 mV s^{-1}; (b) GCD curves at a current density of 0.2 A g^{-1}; (c) specific capacitance as a function of the current densities; (d) Nyquist plots of WW and chemically refined electrodes; and (e) cycling stability of 10DL-AC electrodes in 6 M KOH in a three-electrode system.

chemical refinement (2DL), the specific capacitance reaches up to 71 F g^{-1} at 0.2 A g^{-1}. For 2DL + BL-C and 10DL-C, the specific capacitance increases to 92 F g^{-1} and 98 F g^{-1}, respectively. These results show a 55% improvement in specific capacitance achieved through chemical refinements.

The Nyquist plots are compared in Fig. 6(d) to analyse the resistive and capacitive behaviour of the carbon materials. The semicircles with different sizes indicate their distinct charge transfer resistance, whereas the near-vertical lines show non-ideal capacitive behaviour. The WW-C sample shows a small semicircle in the low Z' region (0.5–0.6 Ω), indicating moderate charge transfer resistance (R_{ct}), reflecting the limited accessibility of active sites due to the unrefined nature of the precursor biomass. The CAC sample, in contrast, has shown a more significant charge transfer resistance. The chemically refined samples have shown distinct trends deviating from those of WW-C. The 2DL-C sample shows a small semicircle indicating reduced R_{ct} and transitioning into a Warburg region where Z'' values increase, reflecting improved ion transport. The 2DL + BL-C sample exhibits a larger, extended semicircle, suggesting a higher R_{ct} than 2DL-C. The 10DL-C sample exhibits a relatively smaller semicircle among the chemically refined samples, showing the lowest charge transfer resistance. This charge transfer resistance is connected to the intrinsic

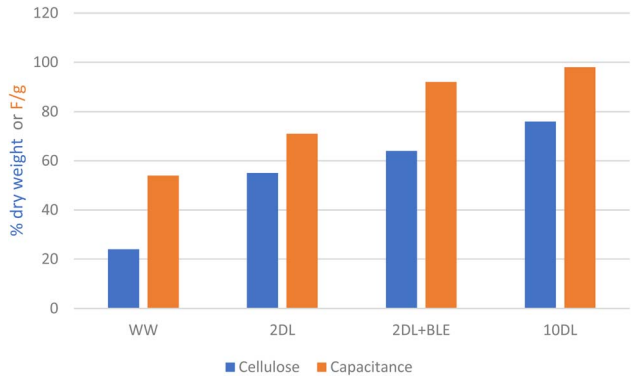

Fig. 7 Influence of chemical refinements on electrochemical performance of carbons: relationship between cellulose content and specific capacitance of supercapacitors with carbon derived from these precursors.

conductivity of electrode materials; the graphitisation level and the total atomic contents of carbon and other heteroatoms are crucial factors.[3]

In both CV analysis and GCD measurements, the 10DL-C shows the highest specific capacitance among the tested samples, probably due to its enhanced graphitic structure, increased surface area (Fig. S4† and Table 3), pore volume, and surface functionalities (as shown in Table 2), all resulting from the chemical refinements to the forage sorghum precursor. During carbonisation, while most oxygen-containing functional groups are decomposed, more stable functional groups remain on the surface of porous carbon. Also, an increase in the π–π^* satellite peak of sp^2 carbon indicates graphitic structure formation contributing to the conductivity of carbon.[42] Such optimal carbon structure formation can be attributed to cellulose enrichment in the biomass precursor,[43] as shown in Fig. 7.

Influence of KOH activation

Since the electrochemical double-layer capacitance (EDLC) mechanism in supercapacitors relies heavily on the available pore volume and surface area on which electrolyte ions develop to form electrical double layers, carbon samples with a larger specific surface area can accommodate a more significant number of charged ions, thereby increasing the specific capacitance. To further enhance the specific surface area and pore volume of the 10DL-C sample, it was activated with KOH treatment. After activating 10DL-C at 800 °C, the resulting activated carbon sample (denoted with 10DL-AC) exhibits a significant increase in pore volume (0.17 $m^3\ g^{-1}$) and surface area (441 $m^2\ g^{-1}$), respectively (Fig. S5†). This expansion of the accessible specific surface area, in combination with the high crystallinity and graphitic structure of 10DL-C, further enhances the electrochemical performance of 10DL-AC.

The electrochemical performances of the 10DL-AC sample are compared with those of the other samples in Fig. 6(a–d). The CV curve of 10DL-AC becomes more quasi-rectangular than that of 10DL-C, enhancing the coulombic efficiency. The GCD measurements indicate that 10DL-AC samples have the longest charge/discharge time. The specific capacitance is increased up to 70%, increasing from 98 F g^{-1} to 140 F g^{-1} at a current density of 0.2 A g^{-1} (Fig. 6(c)). The electrochemical impedance spectroscopic (ECIS) analysis in Fig. 6(d) shows that the 10DL-AC sample has the shortest semicircle, indicating the lowest charge transfer resistance. The short Z'' range reflects efficient ion diffusion through the highly porous structure of 10DL-AC. The electrochemical stability of the 10DL-AC sample for supercapacitor application was further evaluated by cycling it through 5000 consecutive charge–discharge cycles, and it appears suitable for long-term, heavy-duty applications. As shown in Fig. 6(e), the 10DL-AC, the biomass-derived carbon, maintains excellent stability throughout the 5000 consecutive charge–discharge cycles, confirming its robustness for supercapacitor use.

Performance *vs.* sustainability

As discussed earlier, previously reported studies on biomass-derived supercapacitor electrodes focused on manipulating sample preparation conditions during the carbonisation cycle and, more generally, optimising higher maximum furnace temperatures. In contrast, this study demonstrates that precursor chemical refinements can significantly tune the carbon characteristics, offering a novel approach to optimising supercapacitor electrode performance. From a green chemical perspective, the 2DL refinement, which uses a lower concentration of sodium hydroxide, can be relatively preferable due to its reduced chemical use, lower energy consumption, and minimal waste generation. The '2DL'BL' refinement involves treating the pulp with sodium chlorite and acetic acid, effectively producing a white or translucent pulp, although at a low concentration, the elemental chlorine generated during the reaction poses environmental and safety concerns. This method is justifiable in cases where high purity or specific material properties are necessary, provided that proper waste management and recycling practices are in place. In contrast, the '10'DL' refinement is relatively the least sustainable option due to its high chemical consumption (2 kg of NaOH per kg of dry biomass) compared to 2DL (0.4 kg of NaOH per kg of biomass), leading to black liquor waste generation. However, regarding electrochemical performance and comparable carbon yield, the preferential order of chemical refinements for the carbon materials is 10DL > 2DL > 2DL + BL among the investigated methods. As discussed above, 10DL refinement (Fig. 7), compared to other treatments, yields a biomass precursor with high cellulose content and crystallinity and reduced hemicellulose content, making it superior for hard carbon applications. Considering the requirement for precursors with enriched cellulose content and crystallinity for producing hard carbon, chemical refinements for selectively removing hemicellulose and extractives through cleaner and more sustainable pretreatment pathways are recommended for future investigations.

Conclusions

As an example of nonwood lignocellulosic biomass, the sorghum stem part has been investigated to understand the influence of common pulping treatments such as alkali

delignification and bleaching on carbonisation behaviour and structure in connection with energy storage applications. This research reveals that the microstructure, particle size, graphitisation, pore volume, surface area, and surface functional groups of the resultant carbon can be precisely manipulated through controlled chemical refinements of biomass. The cellulose content retained after the treatments strongly influences carbon structure and yield. The 10DL sample with enriched cellulose content exhibited the most promising electrochemical performance among all treated biomass samples. The findings suggest that the electrochemical performance of biomass-derived carbon materials in supercapacitors can be enhanced by selectively removing noncellulosic components or selecting biomass precursors with the desired chemical composition. The removal of extractives generates pores, the elimination of hemicellulose improves the amount of sp^2 bonded carbon, and the presence of cellulose produces more porosity and provides high surface area carbon but yields low carbon. The study offers insights into producing resilient, sustainable, and cost-effective biomass-derived carbon compounds for energy storage applications. For future investigations, exploring more sustainable pretreatment methods that selectively remove hemicellulose and extractives while enriching cellulose content and crystallinity is recommended. These approaches would align better with the principles of green chemistry and offer a cleaner pathway for producing high-performance carbon materials.

Data availability

Data will be made available from authors on request.

Conflicts of interest

There are no conflicts to declare.

Acknowledgements

The author gratefully acknowledges the Australian Government Research Training Program (RTP) scholarship and the University of Queensland's tuition fee offset for supporting this research. The authors gratefully acknowledge the facilities and technical assistance of the Australian Microscopy and Microanalysis Research Facility at the UQ Centre for Microscopy and Microanalysis. This work used the Queensland node of the NCRIS-enabled Australian National Fabrication Facility (ANFF). This work was also supported partly by the Grains Research and Development Corporation (GRDC), the Australian Research Council *via* funding through the ARC Training Centre for Bioplastics and Biocomposites (IC210100023) and the ARC Centre of Excellence for Green Electrochemical Transformation of Carbon Dioxide (GETCO2) (CE230100017). PKA acknowledges financial support from the SIMPLE Hub Regional Research Collaboration (RRC) Program grant from the Department of Education (Australian Government). AKN and JB acknowledge financial support from the Australian Research Council under the ARC Research Hub for Safe and Reliable Energy (IH200100035).

References

1 M. Kim, *et al.*, Efficient lithium-ion storage using a heterostructured porous carbon framework and its *in situ* transmission electron microscopy study, *Chem. Commun.*, 2022, **58**(6), 863–866.
2 B. T. S. Ramanujam, A. K. Nanjundan, and P. K. Annamalai, Chapter 12 – Nanocellulose-based carbon as electrode materials for sodium-ion batteries, in *Nanocellulose Based Composites for Electronics*, ed. S. Thomas and Y. B. Pottathara, Elsevier, 2021, pp. 295–312.
3 M. Kim, *et al.*, Sorghum biomass-derived porous carbon electrodes for capacitive deionization and energy storage, *Microporous Mesoporous Mater.*, 2021, **312**, 110757.
4 W. Wang, *et al.*, Porous carbon nanofiber webs derived from bacterial cellulose as an anode for high performance lithium ion batteries, *Carbon*, 2015, **91**, 56–65.
5 G. Byatarayappa, *et al.*, A comparative study on electrochemical performance of KOH activated carbons derived from different biomass sources - Musa acuminata stem, Pongamia pinnata seed oil extract cake, cajanus cajan stem and Asclepias syriaca floss, *Heliyon*, 2023, **9**(4), e15399.
6 Y. Zhang, *et al.*, Insights into the KOH activation parameters in the preparation of corncob-based microporous carbon for high-performance supercapacitors, *Diamond Relat. Mater.*, 2022, **129**, 109331.
7 S. Saini, P. Chand and A. Joshi, Biomass derived carbon for supercapacitor applications: Review, *J. Energy Storage*, 2021, **39**, 102646.
8 X. Dou, *et al.*, Pectin, Hemicellulose, or Lignin? Impact of the Biowaste Source on the Performance of Hard Carbons for Sodium-Ion Batteries, *ChemSusChem*, 2017, **10**(12), 2668–2676.
9 K. Kepa, Cellulose nanofibre and nanopaper: structure-property-processing relationship and green surface modification, PhD thesis, The University of Queensland, 2021, DOI: **10.14264/027f58a**.
10 J. Hoekstra, *et al.*, Base Metal Catalyzed Graphitization of Cellulose: A Combined Raman Spectroscopy, Temperature-Dependent X-ray Diffraction and High-Resolution Transmission Electron Microscopy Study, *J. Phys. Chem. C*, 2015, **119**(19), 10653–10661.
11 J. Deng, M. Li and Y. Wang, Biomass-derived carbon: synthesis and applications in energy storage and conversion, *Green Chem.*, 2016, **18**(18), 4824–4854.
12 X. Zhou, *et al.*, A Critical Review on Hemicellulose Pyrolysis, *Energy Technol.*, 2017, **5**(1), 52–79.
13 G. Dorez, *et al.*, Effect of cellulose, hemicellulose and lignin contents on pyrolysis and combustion of natural fibers, *J. Anal. Appl. Pyrolysis*, 2014, **107**, 323–331.
14 O. Fromm, *et al.*, Carbons from biomass precursors as anode materials for lithium ion batteries: New insights into carbonization and graphitization behavior and into their correlation to electrochemical performance, *Carbon*, 2018, **128**, 147–163.

15 R. A. Afzal, *et al.*, Lignocellulosic plant cell wall variation influences the structure and properties of hard carbon derived from sorghum biomass, *Carbon Trends*, 2022, **7**, 100168.
16 J. Pennells, Sorghum as a Novel Biomass for the Sustainable Production of Cellulose Nanofibres: An inquiry into Quality, Sustainability, and Statistical Variability in Materials Engineering, *School of Chemical Engineering*, PhD Thesis, The University of Queensland, 2022.
17 A. Lamb, *et al.*, Bioenergy sorghum's deep roots: A key to sustainable biomass production on annual cropland, *GCB Bioenergy*, 2022, **14**(2), 132–156.
18 A. Kanbar, *et al.*, Mining Sorghum Biodiversity—Potential of Dual-Purpose Hybrids for Bio-Economy, *Diversity*, 2021, **13**(5), 192.
19 M. Mujtaba, *et al.*, Lignocellulosic biomass from agricultural waste to the circular economy: a review with focus on biofuels, biocomposites and bioplastics, *J. Cleaner Prod.*, 2023, **402**, 136815.
20 T. N. Silva, *et al.*, Progress and challenges in sorghum biotechnology, a multipurpose feedstock for the bioeconomy, *J. Exp. Bot.*, 2021, **73**(3), 646–664.
21 A. Hosseinmardi, *et al.*, Facile Tuning of the Surface Energy of Cellulose Nanofibers for Nanocomposite Reinforcement, *ACS Omega*, 2018, **3**(11), 15933–15942.
22 N. Amiralian, *et al.*, Easily deconstructed, high aspect ratio cellulose nanofibres from Triodia pungens; an abundant grass of Australia's arid zone, *RSC Adv.*, 2015, **5**(41), 32124–32132.
23 B. Sharma, *et al.*, Chemical composition of processed bamboo for structural applications, *Cellulose*, 2018, **25**(6), 3255–3266.
24 K. H. Kim and C. S. Kim, Recent Efforts to Prevent Undesirable Reactions From Fractionation to Depolymerization of Lignin: Toward Maximizing the Value From Lignin, *Front. Energy Res.*, 2018, **6**, DOI: **10.3389/fenrg.2018.00092**.
25 R. M. Leão, *et al.*, Environmental and technical feasibility of cellulose nanocrystal manufacturing from sugarcane bagasse, *Carbohydr. Polym.*, 2017, **175**, 518–529.
26 S. Tang, *et al.*, PEG-functionalized ionic liquids for cellulose dissolution and saccharification, *Green Chem.*, 2012, **14**(10), 2922–2932.
27 L. Segal, *et al.*, An Empirical Method for Estimating the Degree of Crystallinity of Native Cellulose Using the X-Ray Diffractometer, *Text. Res. J.*, 1959, **29**(10), 786–794.
28 A. Ōya and S. Ōtani, Catalytic graphitization of carbons by various metals, *Carbon*, 1979, **17**(2), 131–137.
29 Y. Wang, *et al.*, Graphene-based solid-phase extraction combined with flame atomic absorption spectrometry for a sensitive determination of trace amounts of lead in environmental water and vegetable samples, *Anal. Chim. Acta*, 2012, **716**, 112–118.
30 T. Adinaveen, *et al.*, Studies on structural, morphological, electrical and electrochemical properties of activated carbon prepared from sugarcane bagasse, *J. Ind. Eng. Chem.*, 2013, **19**(5), 1470–1476.
31 D. Bhattacharjya and J.-S. Yu, Activated carbon made from cow dung as electrode material for electrochemical double layer capacitor, *J. Power Sources*, 2014, **262**, 224–231.
32 M. Sivachidambaram, *et al.*, Preparation and characterization of activated carbon derived from the Borassus flabellifer flower as an electrode material for supercapacitor applications, *New J. Chem.*, 2017, **41**(10), 3939–3949.
33 K. Swennen, C. M. Courtin and J. A. Delcour, Non-digestible oligosaccharides with prebiotic properties, *Crit. Rev. Food Sci. Nutr.*, 2006, **46**(6), 459–471.
34 J. Yu, *et al.*, Cellulose, xylan and lignin interactions during pyrolysis of lignocellulosic biomass, *Fuel*, 2017, **191**, 140–149.
35 H. Yang, *et al.*, Characteristics of hemicellulose, cellulose and lignin pyrolysis, *Fuel*, 2007, **86**(12), 1781–1788.
36 M. Kim, *et al.*, Ultra-stable sodium ion storage of biomass porous carbon derived from sugarcane, *Chem. Eng. J.*, 2022, **445**, 136344.
37 B. S. Santucci, *et al.*, Evaluation of the effects of chemical composition and refining treatments on the properties of nanofibrillated cellulose films from sugarcane bagasse, *Ind. Crops Prod.*, 2016, **91**, 238–248.
38 H. D. Pham, *et al.*, Dual Carbon Potassium-Ion Capacitors: Biomass-Derived Graphene-like Carbon Nanosheet Cathodes, *ACS Appl. Mater. Interfaces*, 2020, **12**(43), 48518–48525.
39 G. Ma, *et al.*, Porous carbon derived from sorghum stalk for symmetric supercapacitors, *RSC Adv.*, 2016, **6**(105), 103508–103516.
40 J. Deng, *et al.*, Effects of Cellulose, Hemicellulose, and Lignin on the Structure and Morphology of Porous Carbons, *ACS Sustain. Chem. Eng.*, 2016, **4**(7), 3750–3756.
41 M. Bora, *et al.*, Blending of Activated Low-Grade Coal Powder with Coconut Shell Waste for Supercapacitor Applications, *Energy Fuels*, 2022, **36**(23), 14476–14489.
42 A. K. Nanjundan, *et al.*, Potassium-Ion Storage in Cellulose-Derived Hard Carbon: The Role of Functional Groups, *Batteries Supercaps*, 2020, **3**(9), 953–960.
43 J. Shi, *et al.*, Direct carbonization of cellulose toward hydroxyl-rich porous carbons for pseudocapacitive energy storage, *Int. J. Biol. Macromol.*, 2024, **264**, 130460.